Design, selection, and characterization of a split chorismate mutase

ARTICLE *in* PROTEIN SCIENCE · MAY 2010

Impact Factor: 2.85 · DOI: 10.1002/pro.377 · Source: PubMed

Design, selection, and characterization of a split chorismate mutase

Manuel M. Müller, Hajo Kries, Eva Csuhai, Peter Kast, and Donald Hilvert*

Laboratory of Organic Chemistry, ETH Zurich, CH-8093 Zurich, Switzerland

Received 23 December 2009; Accepted 2 March 2010
DOI: 10.1002/pro.377
Published online 19 March 2010 proteinscience.org

Abstract: Split proteins are versatile tools for detecting protein–protein interactions and studying protein folding. Here, we report a new, particularly small split enzyme, engineered from a thermostable chorismate mutase (CM). Upon dissecting the helical-bundle CM from *Methanococcus jannaschii* into a short N-terminal helix and a 3-helix segment and attaching an antiparallel leucine zipper dimerization domain to the individual fragments, we obtained a weakly active heterodimeric mutase. Using combinatorial mutagenesis and *in vivo* selection, we optimized the short linker sequences connecting the leucine zipper to the enzyme domain. One of the selected CMs was characterized in detail. It spontaneously assembles from the separately inactive fragments and exhibits wild-type like CM activity. Owing to the availability of a well characterized selection system, the simple 4-helix bundle topology, and the small size of the N-terminal helix, the heterodimeric CM could be a valuable scaffold for enzyme engineering efforts and as a split sensor for specifically oriented protein–protein interactions.

Keywords: protein oligomerization; directed evolution; leucine zipper; split protein; fragment complementation; helix bundle

Introduction

Since the discovery of ribonuclease (RNase) S in the late 1950s,[1] split proteins have made an invaluable contribution to our understanding of protein folding.[2] RNase S is produced by limited proteolysis of ribonuclease A with subtilisin. It consists of a 20 residue N-terminal peptide and a 104 residue C-terminal component. The polypeptides can be separated, and spontaneously refold and assemble into a fully functional enzyme when mixed.[1] The fact that non-covalent interactions between the fragments, both of which are absolutely required for correct folding of RNase S, are sufficient to form an active complex suggests that cooperative interactions are important for folding.[1,2]

Split enzymes permit facile incorporation of synthetic peptide fragments into enzymes, which enabled structure-activity studies long before molecular cloning became a standard method for mutational analysis of proteins.[3] In addition, a wide variety of unnatural building blocks containing photoisomerizable groups,[4] environmentally sensitive dyes,[5] and modified backbones[6] could easily be incorporated into the peptide fragment of RNase S for biophysical studies.

Whereas the fragments of RNase S assemble spontaneously, the affinities of the fragments of most split proteins are not sufficient to guide mutual folding into an active complex. Instead, a dimerization domain attached to the individual protein segments is required to correctly position the subunits, enabling them to fold and function. The necessity for a dimerization mediator allows the use of split proteins as powerful sensors for protein–protein interactions.[7] In protein-fragment complementation

Additional Supporting Information may be found in the online version of this article

Eva Csuhai's current address is Transylvania University, 300 North Broadway, Lexington, KY 40508, USA.

Grant sponsors: ETH Zurich, Swiss National Science Foundation, Stipendienfonds der Schweizerischen Chemischen Industrie (M.M.M.), German Academic Exchange Service (H.K.), Novartis Master Fellowship (H.K.), Oskar Jeger Stipendium, Donors of the American (H.K.), Chemical Society Petroleum Research Fund (E.C.).

**Correspondence to:* Donald Hilvert, Laboratory of Organic Chemistry, ETH Zurich, CH-8093 Zurich/Switzerland. E-mail: hilvert@org.chem.ethz.ch

assays (PCAs), one fragment is fused to a bait, the other to a potential interaction partner or a library of partners (prey), so that a strong interaction between bait and prey leads to activation of the sensor, thereby translating protein–protein interactions into a prominent phenotype. For instance, the gain in catalytic activity upon reassembly of a split dihydrofolate reductase[8] or restoration of fluorescence upon reassociation of split GFP[9] have been employed to investigate leucine zipper domains, among other applications.[10-12] An engineered split ubiquitin system, where assembly leads to proteolytic processing of a fused reporter, has been harnessed to detect interaction partners for transcription factors.[13] Other important applications of split proteins include the study of protein geometries *in vivo*[14] and identification of organelle proteins.[15] Most recently, the Michnick group developed an intriguing life–death strategy based on split-cytosine deaminase to delineate transcriptional networks.[16]

Given the multitude of potential applications of split proteins, extending the repertoire of available tools to include novel members with easily assayable traits, defined fragment affinities, and unique geometries is highly desirable. The AroQ class chorismate mutase (CM) from *Methanococcus jannaschii* (MjCM) offers many features that make it a promising starting point for the generation of a split enzyme. CM catalyzes the Claisen rearrangement of chorismate to prephenate, an essential step in the biosynthesis of aromatic amino acids, providing a facile means to assess enzyme function *in vivo* through complementation assays. Due to its high thermal stability, MjCM offers a robust scaffold for protein redesign.[17,18] The polar active site lies within a helical bundle with residues from four helices contributing to activity. While the fragments of existing split enzymes are typically large, or interact with each other in a complex fashion involving both side chains and the peptide backbone (e.g. RNase S), the helices of helical bundles interact predominantly through their side chains. This feature alleviates some of the constraints on backbone modifications for protein design applications, which is of particular interest given the recent success in constructing helix bundles from nonnatural backbones.[19,20] Here, we present the design, optimization, and characterization of a novel split enzyme based on MjCM.

Results

Design of a heterodimeric chorismate mutase

The interdependence of topology, stability, and enzymatic activity of MjCM, which naturally adopts an all-helical fold and assumes a domain-swapped dimer configuration, has been studied extensively.[18,21-24] Insertion of short peptide sequences into the middle of the dimer-spanning N-terminal helix converts the natural homodimer into monomers (mMjCM),[18] trimers,[22] and hexamers.[22] The tolerance of the N-terminal helix to disruption between residues 21 and 22 also makes this an attractive cleavage site for the generation of a heterodimeric mutase [Fig. 1(A)].

To test whether the activity of the C-terminal fragment consisting of helices H1b, H2, and H3 could be reconstituted upon addition of the N-terminal helical segment H1a (H1a contains the essential active site residue Arg9), we prepared both components. The N-terminal peptide comprising residues 1–20 ($MjCM_{1–20}$) was prepared by solid-phase peptide synthesis (SPPS) methods, and purified by HPLC. The C-terminal portion containing the additional mutation I77R to disfavor homodimerization[18] ($MjCM^*_{22–93}$) was produced by heterologous expression in the CM-deficient *Escherichia Coli* strain KA13[27] with a C-terminal His_6-tag and purified on a Ni-NTA column. However, mixing the components at equimolar concentrations (0.1 μM) produced no significant CM activity *in vitro* (data not shown). Furthermore, when the genes for $MjCM^*_{22–93}$ and a representative variant (Glu3Gly) of $MjCM_{1-21}$ were subcloned into the selection plasmid pMG211[28] (yielding pMG211B_split, see Materials and Methods), coexpression in the CM-deficient *E. coli* selection strain KA12/pKIMP-UAUC[29] did not allow for growth on selective agar plates lacking phenylalanine and tyrosine (Supporting information Fig. 1).

To facilitate heterodimerization of $MjCM_{1–21}$ and $MjCM^*_{22–93}$, engineered antiparallel Leu-zippers (*NZ* and *CZ*)[30] were attached to the C-terminus of $MjCM_{1-21}$ and to the N-terminus of $MjCM^*_{22–93}$, respectively, in analogy to the strategy employed by Ghosh *et al.*[30] in the construction of split-GFP. Due to its antiparallel orientation, this coiled-coil dimerization domain serves as a simple, noncovalent mimic of the peptide hinge loop of mMjCM.[18] The domains were connected by flexible glycine-rich linkers, resulting in $MjCM_{1-21}$-GGSGSG-*NZ*-His_6 (referred to as N1-Z) and *CZ*-GGSG-$MjCM^*_{22–93}$-His_6 (referred to as Z-C3) as shown in Figure 1(B). When N1-Z and Z-C3 were coproduced in the same cell, the CM deficiency could be complemented, albeit poorly (data not shown). Similarly, when N1-Z and Z-C3 were coproduced and purified under native conditions, low levels of mutase activity were observed. The k_{cat}/K_m value for N1-Z·Z-C3 was estimated to be 80 $M^{-1}s^{-1}$ (Supporting information Fig. 2), which is more than two orders of magnitude lower than that of mMjCM under similar conditions ($k_{cat}/K_m = 1.9 \times 10^4$ $M^{-1}s^{-1}$ at 20°C).[18]

Selection of improved variants

The low levels of CM activity exhibited by N1-Z·Z-C3 prompted us to optimize the split enzyme by combinatorial mutagenesis and *in vivo* selection. We replaced the glycine and serine-rich linkers with two

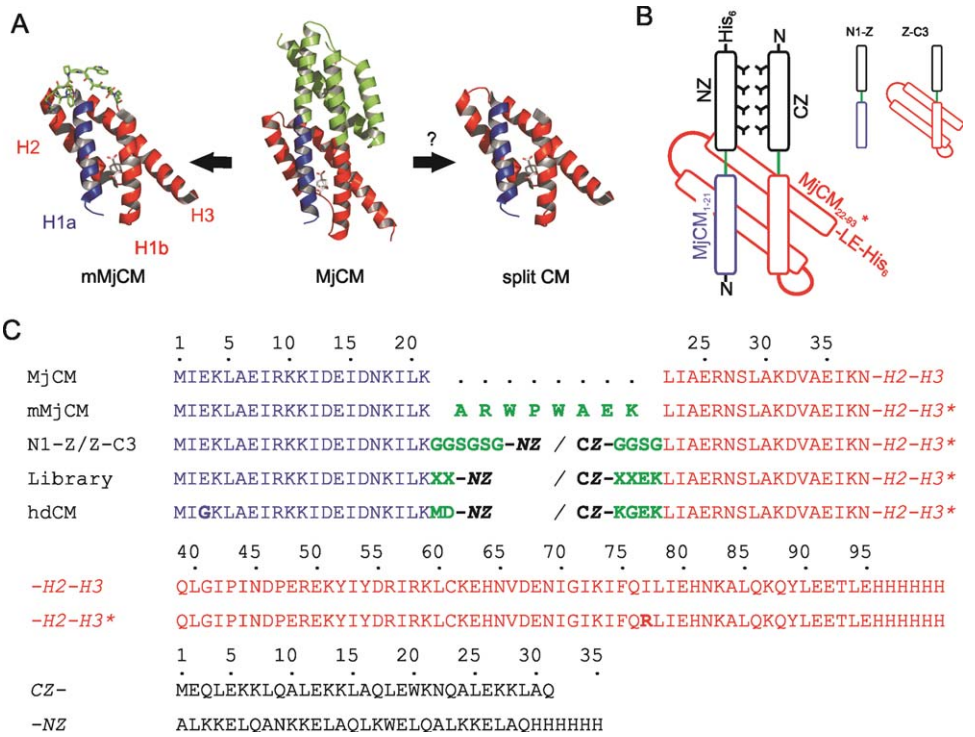

Figure 1. Structures and sequences of CM variants. (A) Ribbon diagrams of the natural AroQ class dimer (MjCM, represented by a homologous enzyme from *E. coli*, for which a crystal structure has been determined; PDB code 1ecm[25]), the engineered monomer (mMjCM,[18] PDB code 2gtv[26]), and the model of the designed split CM. (B) Schematic representation of hdCM and its subunits. (C) Sequence alignment of CM variants and sequences of Leu zipper peptides. X stands for any of the 20 proteinogenic amino acids. Helix H1a, encompassing residues 1–21, is depicted in blue, residues $MjCM_{22–93}$ in red, linker regions in green, and leucine zipper dimerization domains in black.

random amino acids in N1-Z and an X-X-E-K linker (where X denotes any standard amino acid) in Z-C3 [Fig. 1(C)]. This linker design would permit formation of a continuous helix extending from the mutase segment to the leucine zipper, as well as kinks or more flexible connections between the helical fragments. The length was chosen to allow the hydrophobic faces of the leucine zippers to interact should continuous helices be formed. In addition, short linkers might better promote CM assembly upon leucine zipper dimerization than the long flexible linker of the original N1-Z design. The charged glutamate and lysine residues in Z-C3 were retained from the design of mMjCM.[18]

The genes for both polypeptides were assembled by overlap extension PCR from a plasmid encoding N1-Z·Z-C3 with randomized primers, and ligated into a derivative of pMG211[28] (Supporting information Fig. 3). The library was transformed into the selection strain and aliquots were plated on rich medium agar plates to evaluate library size and quality. The library contained roughly 4.5 x 10^5 members, approximately 2–3-fold more than the number of theoretical possibilities for four randomized amino acid positions. Twelve clones were sequenced to assess the diversity of the library. One of these contained the original N1-Z·Z-C3 sequence, presumably reflecting a contamination from undigested vector. Although the codon distribution of the randomized linker was slightly biased due to an overrepresentation of T vs C in the synthetic oligonucleotides (Supporting information Table I), the range of amino acid substitutions observed appeared to be broad. We subjected an aliquot of the library containing 10^3-10^4 variants to selection for phenylalanine and tyrosine prototrophy. Of these, almost 400 clones were found to complement the CM deficiency. Of twelve complementers chosen for sequencing, eight represented contamination from the original N1-Z·Z-C3 design, which thus appears to be superior to many mutated library members. However, the remaining four variants were highly active clones with a distinct set of linker sequences composed of a roughly equal number of polar (Asp, Asn, Ser, His, Lys, Arg) and nonpolar (Gly, Ala, Pro, Leu, Met) residues (Table I). Clone 30S formed particularly large colonies on selective plates, and was therefore chosen for further analysis. It codes for the fragments $MjCM_{1\text{-}21(+E3G)}$-MD-*NZ*-His_6 and *CZ*-KGEK-$MjCM^*_{22–93}$-His_6, which will be referred to as hdN1 and hdC3, respectively. The corresponding heterodimeric complex is designated as hdCM [Fig. 1(C)].

Production and purification

For biophysical characterization of the selected heterodimer, the genes encoding hdN1 and hdC3 were

Table I. *Linker Sequences of Selected Clones*[a]

	N1-Z-linker		Z-C3-linker	
Clone	DNA sequence	Protein sequence	DNA sequence	Protein sequence
30S	ATG GAC	Met Asp (+E3G)	AAA GGC	Lys Gly
38S	ACC CCA	Ser Pro	CCT AAC	Pro Asn
40S	AAT GAT	Asn Asp (+E3G)	CAC TTG	His Leu
42S	GCG CCT	Ala Pro	AGA GCA	Arg Ala

[a] Additional mutations outside of the randomized stretch are indicated in parentheses, with residue numbering according to MjCM.

subcloned from the library construct into separate pMG211 vectors. The enzyme fragments were produced separately in CM-deficient KA13 cells[27] and purified by Ni-NTA chromatography and reverse-phase HPLC. Purity and mass of the fragments were confirmed by analytical HPLC (Supporting information Fig. 4) and LC-MS (hdN1 calculated: 7154.4 Da, found: 7154 Da; hdC3 calculated: 13759.8 Da, found: 13760 Da). After HPLC purification, 13 and 9 mg of pure lyophilized protein were obtained per liter of cell culture for hdN1 and hdC3, respectively.

Activity of individual subdomains and hdCM

As both fragments of hdCM contain essential active site residues, individual fragments alone were anticipated to be inactive. To verify this assumption, *in vitro* activity and *in vivo* complementation of the separated fragments were tested. As expected, the genes encoding the individual fragments of the evolved hdCM expressed from plasmids did not complement the CM deficiency on selective agar plates (Supporting information Fig. 1). Clones producing only hdN1 showed irregular growth on nonselective plates suggesting toxic effects of the peptide [Supporting information Fig. 1(B)]. *In vitro*, the hdN1 and hdC3 fragments showed reaction rates that were not significantly above the background rate. The k_{cat}/K_m value of $\leq$ 0.3 $M^{-1}s^{-1}$ measured for hdC3 at 10 μM concentration is at least two orders of magnitude lower than that of a crippled *E. coli* CM lacking the active site arginine of the N-terminal helix (R11A EcCM k_{cat}/K_m = 30 $M^{-1}s^{-1}$).[31] This further reduction in activity compared to the point mutant, which is roughly four orders of magnitude less active than wild-type mutases, shows that the absence of the N-terminal helix seriously compromises the integrity of the hdCM active site.

In contrast, when 0.1 μM hdC3 was provided with a 50-fold excess of hdN1, activities rivaling those of natural CMs were obtained (Fig. 2). The steady-state parameters at 25°C and pH 6.5 are k_{cat} = 5.3 ± 0.8 s^{-1} and K_m = 112 ± 25 μM, which compares favorably with the kinetic parameters for wild-type MjCM (k_{cat} = 5.7 s^{-1} and K_m = 41 μM at 30°C).[32]

Biophysical characterization

Far-UV circular dichroism spectra were recorded for the individual fragments and the heterodimer [Fig. 3(A)]. At 10 μM, both fragments are helical even when separated. Upon dimerization, a small change in intensity was observed, with the resulting spectrum of the complex being similar to that reported for MjCM.[32]

Analytical ultracentrifugation (AUC) measurements were performed to analyze the oligomerization behavior of the split CM and its fragments [Fig. 3(B)]. In sedimentation equilibrium measurements at 4 μM of hdN1, hdC3, or hdCM, the traces fit to species with molecular masses of 14.9 kDa (hdN1), 25.8 kDa (hdC3) and 23.4 kDa (hdCM). The observed masses roughly correspond to homodimers of hdN1 (14.3 kDa calc.) and hdC3 (27.5 kDa calc.) in the absence of the complementary binding partner, and to a heterodimer of hdN1 and hdC3 when both fragments are present (hdCM, 20.9 kDa calc.). However, the presence of multiple species and their complex equilibria preclude a simple determination of dissociation constants for the dimers from the available data.

To determine the affinity of the engineered mutase fragments for each other, we titrated the fragments and deduced complex formation from kinetic activity. By adding increasing amounts of hdN1 to

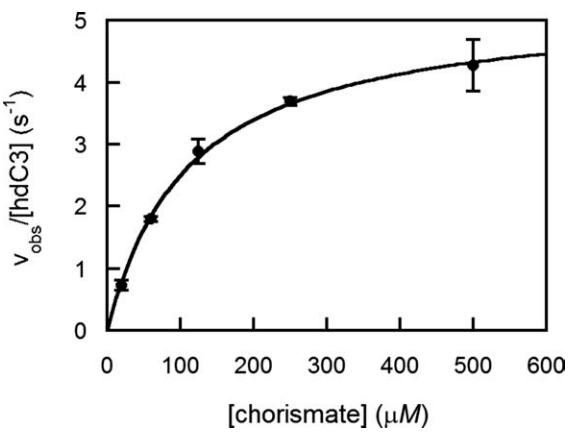

Figure 2. Michaelis-Menten kinetics of hdCM. Initial velocities were determined at 0.1 μM hdC3 with a 50-fold excess of hdN1 at pH 6.5 and 25°C.

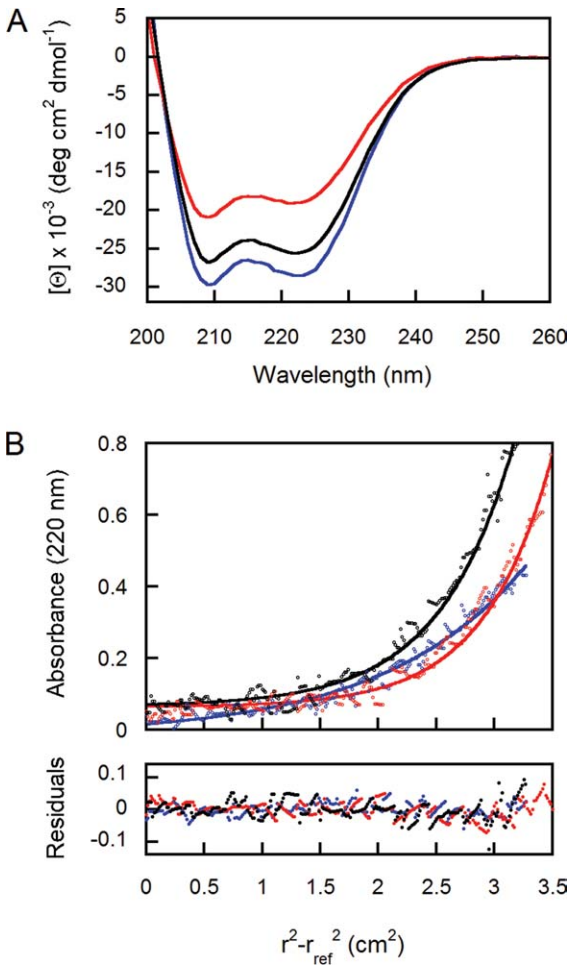

Figure 3. Secondary and quaternary structure of hdCM. (A) Far-UV CD spectra of hdCM and its fragments. Spectra were recorded at 10 μ*M* concentration of the separate fragments (hdN1 in blue; hdC3 in red) or of the complex (hdCM in black). (B) Analytical ultracentrifugation of hdCM and its subunits. Sedimentation equilibrium data were recorded at 4 μ*M* each of hdCM (black), hdN1 (blue) and hdC3 (red). For clarity, only traces at 35,000 rpm are shown. The curves represent fits to a single-species model. Residuals are displayed in the lower panel. Similar fits were obtained at lower speeds.

0.1 μ*M* hdC3 and measuring CM activity, a K_d of 310 ± 90 n*M* was obtained (Fig. 4).

Insertion of a hinge loop into the dimer-spanning H1 helix of MjCM dramatically reduced its stability, yielding a monomeric molten globule.[33] To compare the stability of hdCM with its congeners, we performed thermal and chemical denaturation experiments. Thermal denaturation at 2 μ*M* hdCM [Fig. 5(A)] indicated that unfolding was cooperative with a midpoint of transition at approximately 73°C. In contrast, the wild-type dimer MjCM unfolds highly cooperatively with a transition at 88°C under similar conditions,[32] while the monomeric mutase (mMjCM) unfolds without cooperativity (the unfolding of mMjCM becomes modestly cooperative with a

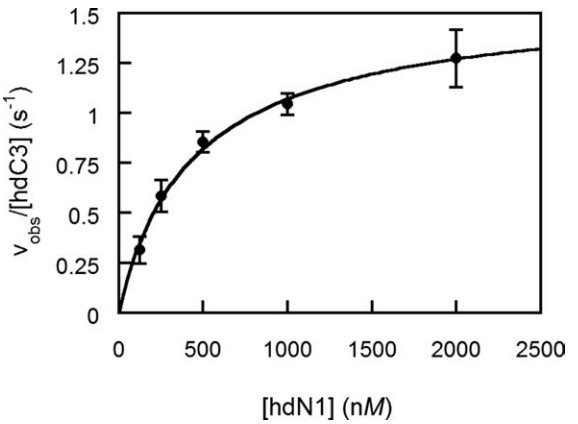

Figure 4. Dimerization of hdCM fragments. The activity of hdCM was followed upon titration of 0.1 μ*M* hdC3 with hdN1. A K_d value of 310 ± 90 n*M* (error of the fit is indicated) was obtained by fitting the data to Eq. 1 of the Materials and Methods section.

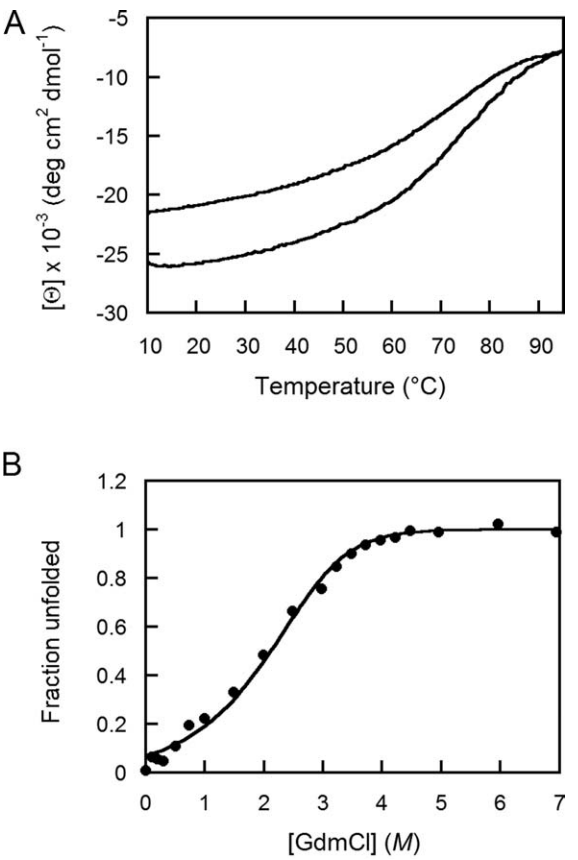

Figure 5. Stability of hdCM. (A) Thermal denaturation of 2 μ*M* hdCM monitored by CD spectroscopy at 222 nm. The lower trace corresponds to denaturation during heating, the upper trace to renaturation upon cooling. The midpoints of the unfolding and refolding transitions, determined by smoothing of curves and taking the first derivative, both lie at 73°C. (B) Chemical denaturation of 2 μ*M* hdCM. In a titration with GdmCl, the mean residue ellipticity was followed by CD spectroscopy at 222 nm. Small deviations from an ideal two-state model of unfolding can be observed, similar to the deviations obtained for MjCM[32] and variants thereof.[34]

Table II. *Stability of Chorismate Mutases*[a]

Protein	$\Delta G_U^0(H_2O)$ (kcal/mol)	m (kcal/mol·M)	ΔG_{diss} (kcal/mol)	K_d (μM)
hdCM	10.5 ± 0.1	1.3 ± 0.1	8.9	0.3
mMjCM[34]	2.8 ± 0.1	0.69 ± 0.02	–	–
MjCM[34]	28 ± 1	5.0 ± 0.2	n.d.	n.d.
NZ/CZ[9]	n.d.	n.d.	6.4	20
$MjCM_{1-21}/MjCM^*_{22-93}$[b]	n.d.	n.d.	2.5	15,000

[a] CMs were denatured with GdmCl (MjCM and hdCM) or urea (mMjCM). Data were fit to a dimeric model (hdCM and MjCM)[32] and to a monomeric model (mMjCM).[18] The error of the fit is indicated. $\Delta G_U^0(H_2O)$ represents the free energy of unfolding extrapolated to water, m is the slope of a plot of [GdmCl] vs ΔG_U^0. Parameters for mMjCM and MjCM were taken from Woycechowsky *et al.* (ref 34). Dissociation constants (K_d) were determined through kinetic titrations for hdCM (this work), and by surface plasmon resonance for the coiled-coil alone (*NZ/CZ*).[9] n.d., not determined.
[b] The affinity of the CM fragments for each other was estimated by subtracting the dissociation energy of the leucine zipper domain from the dissociation energy of hdCM.

transition at 55°C in the presence of a transition state analog inhibitor[33]). The greater stability of hdCM compared to the monomer was confirmed by chemical denaturation with GdmCl [Fig. 5(B)]. The free energy of unfolding $\Delta G_U^0(H_2O)$ obtained for hdCM (10.5 kcal/mol) is considerably higher than that of mMjCM (2.8 kcal/mol)[34] but still far lower than that of MjCM (28 kcal/mol)[34] (Table II). This value corresponds reasonably well with the dissociation energy determined from the kinetic affinity measurements (8.9 kcal/mol). Assuming that the binding energies of the individual subdomains are additive, the dissociation energy for the CM portion can be calculated by subtracting ΔG_{diss} of the free leucine zipper (6.4 kcal/mol; taken from reference 9) from ΔG_{diss} of hdCM, yielding a contribution of the CM portion to dimerization of only 2.5 kcal/mol (Table II). This value is comparable to the stability reported for mMjCM.[34]

1-Anilinonaphthalene-8-sulfonate (ANS) exhibits a strong solvatochromic effect (blue-shift of emission, increase of fluorescence yield) upon transfer from aqueous solution to readily accessible hydrophobic patches of proteins, and has therefore been used to assess the tightness of packing in hydrophobic cores.[35] The changes in ANS fluorescence upon binding to hdCM resemble those observed with mMjCM with respect to the increase in intensity and the shift of the emission maximum, indicating that hdCM retains some properties of a molten globule. In contrast, no change in signal was observed upon addition of ANS to hdN1, presumably due to the lack of hydrophobic pockets in the peptide. The ANS binding of hdC3 was significant, but much weaker than that for the heterodimer (Fig. 6).

Discussion

Natural and engineered enzymes with distinct folds and various multimeric topologies can efficiently catalyze the rearrangement of chorismate to prephenate.[18,22-24,36-38] Here we show for the first time the construction of a functional *hetero*dimeric CM. Simply cleaving the dimer-spanning N-terminal helix of MjCM to yield a one-helix and a three-helix fragment abolishes enzyme function *in vitro* and *in vivo*. However, attaching a leucine zipper dimerization domain to the two polypeptides and optimizing the linker sequences using *in vivo* selection from randomized libraries yielded a variant (hdCM) with wild-type like activities. While the individual fragments of hdCM are inactive, they assemble with submicromolar affinities to a fully active complex. The success of this approach indicates that optimization of linker sequences by directed evolution might be suitable as a general strategy to develop novel heterodimeric protein complexes.

Reconstitution of a functional enzyme via an external dimerization domain in this way is potentially useful for diverse applications. For example, split proteins are valuable tools for the detection and characterization of noncovalent interactions.[7] For the high-throughput detection of protein complexes, PCAs rely on the generation of a fluorescent signal or an enzymatic activity coupled to host survival upon assembly. Fluorescence detection allows experiments to be conducted *in vitro*, making

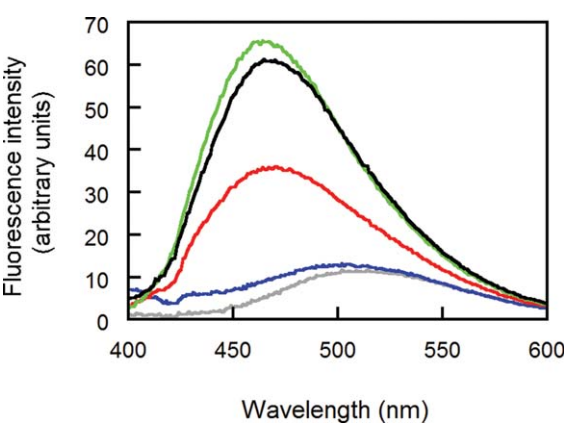

Figure 6. ANS binding of CM variants. The fluorescence spectra of 2 μM ANS were recorded in the presence of 2 μM hdN1 (blue), hdC3 (red), hdCM (black), and mMjCM (green), and in the absence of protein (gray) using an excitation wavelength of 370 nm. MjCM does not bind ANS to an appreciable extent.[33]

virtually any noncovalent interaction amenable to screening.[39] On the other hand, *in vivo* selection experiments enable the simultaneous interrogation of much larger libraries of potential protein–protein interaction partners. The CM selection system is particularly well characterized, making the split CM a potentially useful addition to the toolkit of split sensors. The ability to adjust the stringency of the CM selection system with tightly regulatable promoters and specific degradation tags that control protein levels[40] could be advantageous, as it provides a simple means of fine-tuning the dynamic range of interactions that can be assayed.

The relative orientation of possible interaction partners distinguishes individual split proteins. For example, split-DHFR is assembled via fusion partners attached to the N-termini of both fragments,[41] whereas hdCM, like split-GFP,[30] is dimerized by a domain fused to the N-terminus of one segment and the C-terminus of the other. Whereas typical split sensors are connected to their probes by flexible linkers, the short, optimized hdCM linkers add a stringent geometric constraint to the mode of dimerization, rendering hdCM particularly suitable for investigations of specifically oriented protein-protein interactions. For instance, hdCM is expected to strictly distinguish antiparallel and parallel coiled-coils, and maybe sense differences in supercoiling. This system is presumably not restricted to probing coiled-coil interactions, however. The original split CM design with flexible linkers complemented the CM deficiency *in vivo*, albeit weakly, and could conceivably be adapted for detection of a wider range of interaction partners. The use of flexible linkers would relax the geometric constraints, although efficient complementation will clearly require high affinity dimerizing agents.

As for a few other split proteins, including several GFP variants[42] and RNase S,[1] the small size of the N-terminal H1a helix should facilitate synthetic control of structure and function. CM is an important model enzyme,[43] and its mechanism can now be systematically probed with greater ease by replacing the N-terminal segment with synthetic peptides.[44] The topological simplicity of four-helix bundles also makes this system attractive as a starting point for the creation of artificial catalysts. Specifically, synthetic versions of the N-terminal helix would be ideally suited to deliver diverse functional groups to the CM active site. Formation of functional heterodimers will take advantage of the spatial separation of affinity, mediated by coiled-coil formation, and activity, localized at the catalytic pocket of the enzyme. Replacement of H1a with helix surrogates constructed from nonnatural building blocks[19,20,45] could also give rise to novel hybrid enzymes. Such systems could be optimized through combinatorial analysis of small libraries of both the synthetic and the recombinant fragment, again taking advantage of noncovalent assembly of the leucine zipper to bring the two components into proximity.

Materials and Methods

E. coli *strains*

E. coli strains KA12 (genotype: Δ(*srlR-recA)306:* Tn*10*, Δ(*pheA-tyrA-aroF), thi-1, endA-1, hsdR17,* Δ*(argF-lac)U169, supE44*),[29] and XL1-Blue (Stratagene) were used for cloning purposes. KA13, a derivative of KA12 carrying a T7 RNA polymerase[27] was used for protein production, and KA12/pKIMP-UAUC[29] for *in vivo* selection experiments.

Molecular cloning

Nucleic acid manipulations were performed following standard procedures.[46] Plasmids were purified with JETquick kits on a miniprep or midiprep scale (Genomed). DNA concentrations were measured with a NanoDrop spectrophotometer (Witec AG). DNA sequencing was performed using the flanking primers T7 and T7TR and the Big Dye Terminator v3.1 sequencing mix on a 3100-Avant Genetic Analyzer (Applied Biosystems). All primers, synthesized and purified by Microsynth, are listed in the Supporting information (Supporting information Table II).

Plasmids

All plasmids constructed in this work are depicted schematically in the Supporting information (Supporting information Fig. 5). pMG211-mMjCM was prepared by ligating the 4561 bp *Nde*I-*Xho*I fragment of pMG211[28] and the 306 bp *Nde*I-*Xho*I fragment of pET-mMjCM′, which was constructed by inserting the sequence for the selected monomer into pET22b(+)[18] (Andreas Kleeb, unpublished). The DNA fragment for the truncated $MjCM_{22–93}$ was amplified from pMG211-mMjCM using primers CM2293f and CM2293r and digested with *Nde*I and *Spe*I yielding a 225 bp fragment, which was ligated into the 4529 bp fragment from *Nde*I and *Spe*I-digested pMG211_mMjCM, yielding pMG211_mMjCM$_{22–93}$. All other plasmids are derived from pMG211B_N1-ZZ-C3; its map and sequence are shown in Supporting information Figure 5. Briefly, pMG211B_N1-ZZ-C3 was constructed as follows: PCR-amplified CM gene fragments (originally stemming from pMG211_mMjCM, unpublished) were furnished with sequences for leucine zippers and flexible linkers using PCR and were ligated into pMG211. A *Bam*HI restriction site was introduced into this intermediate by quick change mutagenesis using primers BamHIf and BamHIr, resulting in pMG211B_N1-ZZ-C3. pMG211B_hdCM was isolated from library clone 30S; the assembly of the library plasmids is described below. For pMG211_hdN1, the *hdN1* gene was amplified from pMG211B_hdCM with the

primers N1-ZXhoI_r and N1-ZNheI_f. These primers introduced an N-terminal *Nhe*I site, and a *Sac*I site close to the C-terminus by silent mutation, and an *Xho*I site upstream of the sequence of the His_6-tag linking it to the C-terminus by leucine and glutamate. The 174 bp PCR product was ligated into pMG211 via the *Xho*I and *Nde*I sites. For pMG211_hdC3, the *hdC3* gene was amplified from pMG211B_hdCM with the primers A1-Xr and T7, and ligated into the pMG211 vector via an *Nde*I and an *Xho*I site. pMG211B_split was constructed by subcloning a PCR product of pMG211B_hdCM using primers split_r and split_f via *Bam*HI and *Xba*I sites (443 bp) into the 4490 bp fragment of *Bam*HI- and *Xba*I-digested pMG211B_N1-ZZ-C3. In so doing, the gene encoding the N-terminal helix of CM not only lost the Leu zipper domain but also its His_6-tag. All plasmids bear a dual promoter system enabling regulated moderate gene expression using P_{sal} for *in vivo* selection experiments and strong expression for protein production from P_{T7}.[47]

Library construction

The linker library was constructed based on pMG211B_N1-ZZ-C3 (Supporting information Fig. 5). This plasmid served as template for PCR amplification of three fragments with the primer pairs T7/C3-Xr, C3-Xf/N1-Xr, and N1-Xf/T7TR (Supporting information Fig. 3 and Supporting information Table II). N1-Xf and C3-Xf were randomized at six nucleotide positions. PCRs were carried out with approximately 1 ng/μL plasmid, 0.2 μ*M* of each primer, 0.2 m*M* of each dNTP, and 50 U/mL *Taq* polymerase in 1x *Taq* buffer (New England Biolabs). Following an initial denaturation (96°C for 120 s), amplification was carried out over 28 cycles (95°C for 30 s, 50°C for 30 s, 72°C for 60 s) and ended with a final elongation (72°C for 300 s). Products were separated by agarose gel electrophoresis and extracted with NucleoSpin Extract II kits (Machery-Nagel). The fragments were assembled using PCR by subjecting the three fragments to four amplification cycles, then adding the flanking primers T7 and T7TR and performing 30 more amplification cycles. The resulting 810 bp fragment was again amplified by PCR, digested with *Bam*HI and *Xba*I (656 bp) and ligated to the 4490 bp fragment of *Bam*HI- and *Xba*I-digested pMG211B_N1-ZZ-C3. The ligated 5146 bp library plasmids were purified by phenol/chloroform extraction, washed with Tris-HCl, pH 8.0, in a YM-30 Millipore Microcon filter, and concentrated to approximately 0.3 μg/μL. Then, 1 μg DNA was transformed into electrocompetent KA12/pKIMP-UAUC cells. Transformed cells were taken up in 18 mL SOC medium and incubated at 30°C and 170 rpm for 50 min. The library size was determined by plating an aliquot from this cell suspension on unselective LB agar plates containing 150 μg/mL sodium ampicillin (amp) and 30 μg/mL chloramphenicol (cam). Amp and cam were added to the remaining bacterial suspension and the library was grown overnight at 30°C. From this overnight culture, a glycerol stock was taken (30% glycerol) and frozen at −80°C.

In vivo *complementation experiments*

CM complementation experiments were performed according to previously published procedures.[29] Briefly, KA12/pKIMP-UAUC cells harboring target plasmids (pMG211B_hdCM, pMG211B_split, pMG211_mMjCM, pMG211_clone42S, pMG211_hdN1, pMG211_hdC3 or the plasmid library) were plated on M9c-agar plates[47] containing 100 μg/mL amp, 20 μg/mL cam, 60 μ*M* IPTG (promoting gene expression from the helper plasmid pKIMP-UAUC), and 10 μ*M* salicylate (to induce CM production) in the presence or absence of 20 μg/mL L-tyrosine and L-phenylalanine. For *in vivo* selection of library clones, 5 mL LB amp/cam were inoculated with 50 μL of the glycerol stock and incubated until an OD_{600} of 1 was reached. Cells were then washed two to three times with M9 salts, and appropriate dilutions in M9 salts were plated.

Solid-phase peptide synthesis

$mMjCM_{1\text{-}20}$ was synthesized on a Wang resin preloaded with Fmoc-Leu (0.68 mmol/g) on a 433A peptide synthesizer (Applied Biosystems) on a 0.1 mmol scale with standard Fmoc-protected amino acids (Novabiochem). The peptide was cleaved from the resin and amino acid protecting groups were removed by incubation in 95% TFA, 2.5% H_2O, and 2.5% TIS for 2 h. The resin was filtered off, excess TFA was evaporated, and the peptide was precipitated and washed with cold ether and dried under vacuum. The peptide was purified by two rounds of preparative HPLC with a linear gradient of 5–85% acetonitrile (0.05% TFA) in water (0.1% TFA). Peptide masses were analyzed by LC-MS with an Atlantis T3 chromatography column (Waters) and an ESI ion source (Finnigan LCQ Deca).

Protein production

Flasks containing 500 mL LB medium with 150 μg/mL amp were inoculated with 1–2 mL of a dense overnight culture of KA13[27] cells containing a plasmid encoding the appropriate CM gene (pMG211B_N1-ZZ-C3, pMG211_hdN1, or pMG211_hdC3). The cells were incubated at 37°C and 230 rpm until an OD_{600} of 0.6–0.8 was reached. Gene expression from the T7 promoter was induced with IPTG at a final concentration of 0.25 m*M* and incubation was continued for approximately 20 hours at 37°C. Cells were harvested by centrifugation, and the cell pellet was resuspended in 10 mL PBS (50 m*M* NaH_2PO_4, pH 6.5, 160 m*M* NaCl) containing a spatula tip of lysozyme and DNase I. After 30 min on ice, protease

inhibitors were added (final concentrations: 1 μg/mL pepstatin, 5 μg/mL aprotinin, 5 μ*M* PMSF), and cells were lysed by sonication. After removing cell debris by centrifugation at 4000 g and 4°C for 20 min, the cleared lysate was purified by Ni-NTA (Sigma) chromatography. His-tagged proteins were eluted with 10 m*M* phosphate, pH 6.5, containing 160 m*M* NaCl and 250 m*M* imidazole. Protein-containing fractions were pooled and used directly for assays after dialysis against PBS in the case of N1-Z and Z-C3. hdN1 and hdC3 were further purified by preparative HPLC on a Nucleosil 100–7 C18 column (Machery-Nagel) with a gradient of 5–60% acetonitrile (0.05% TFA) in water (0.1% TFA). Protein-containing fractions were lyophilized, dissolved in 10 m*M* TFA and stored in glass vials. Protein masses were confirmed by LC-MS as described above. Protein concentrations were determined by measuring the absorbance at 280 nm on a NanoDrop spectrophotometer (Witec AG) with calculated extinction coefficients (hdN1: 5,500 $M^{-1}cm^{-1}$, hdC3: 9,970 $M^{-1}cm^{-1}$).

Kinetic assays

Kinetic assays were conducted by measuring the consumption of chorismate at either 274 nm (ε = 2630 $M^{-1}cm^{-1}$) or 310 nm (ε = 370 $M^{-1}cm^{-1}$) with a UV-VIS spectrophotometer (Perkin-Elmer Lambda 35) according to previously published procedures.[28] All measurements were performed in PBS at pH 6.5 and 25°C in the presence of 0.1 mg/mL BSA. For Michaelis-Menten kinetics at 0.1 μ*M* enzyme concentration, hdCM was preequilibrated as a 10 μ*M* stock solution in the presence of 1 mg/mL BSA in PBS, pH 6.5, in a 1.5 mL Eppendorf tube for several minutes. For measurement, the premix was added to the temperature-equilibrated cuvette containing buffer and 20 μ*M* to 3 m*M* chorismate.

A dissociation constant of hdCM was determined from a plot of v_{obs}/[hdC3] against the concentration of hdN1 at 0.1 μ*M* concentration of hdC3. v_{obs} was calculated from initial velocities at 50 μ*M* chorismate, measured under standard kinetic assay conditions in duplicate. The hyperbolic binding curve was fit nonlinearly to the dimeric binding model according to Equation 1:

$$\frac{v_{obs}}{[hdC3]} = c\left\{\frac{[hdN1]+[hdC3]+K_d}{2} - \sqrt{\frac{([hdN1]+[hdC3]+K_d)^2}{4} - [hdN1][hdC3]}\right\} \quad (1)$$

where c is a constant relating the concentration of the dimer hdCM to the activity, [hdN1] is the initial concentration of hdN1, [hdC3] the initial concentration of hdC3 and K_d the dissociation constant of the heterodimer.

Analytical ultracentrifugation

Analytical ultracentrifugation was performed on a Beckman XL-A analytical ultracentrifuge equipped with an An-60Ti rotor. hdCM and its fragments were measured at 4 μ*M* concentration in PBS. Sedimentation equilibrium experiments (SE) were performed using six-channel charcoal-epon cells with quartz windows. The time to reach equilibrium was estimated using Ultrascan and monitored by subtracting two scans which were taken 4 h apart. Three scans per cell were recorded using 0.001 cm point spacing and averaging 10 readings per point at 220 nm after equilibrium was reached. SE was performed at 15,000, 20,000, 25,000, 30,000, and 35,000 rpm at 25°C. The density of the buffer was measured at 25°C using a DSA48 density and sound analyzer (Anton Paar). The partial specific volume of each protein was calculated using the program Sednterp.[48] Data analysis was performed using Ultrascan v. 6.2.[49] The data were fit to an ideal single-species model using Equation 2:

$$A_r = exp\left\{ln(A_0) + \left(M[1-\bar{\nu}\rho]\frac{\omega^2}{2RT}\right)(x^2 - x_0^2)\right\} + E \quad (2)$$

where A_r is the absorbance at radius x, A_0 the absorbance at a reference radius x_0 (the meniscus), M the molecular weight of the single species, $\bar{\nu}$ the partial specific volume of the protein, ρ the density of the solvent, ω the angular velocity, R the universal gas constant, T the temperature, and E the baseline error correction factor.

CD spectroscopy

Far-UV CD spectra of protein samples were recorded at 25°C on an Aviv 202 spectropolarometer from 200 to 260 nm in 1 nm steps with an averaging time of 2 s in PBS at 10 μ*M* protein concentration. Three scans were averaged and a PBS blank was subtracted. A thermal denaturation curve was obtained by measuring ellipticity of a 2 μ*M* protein solution at 222 nm between 10 and 95°C. After a 10 min initial equilibration at 10°C, the sample was heated at a rate of 1°C/min in 0.5°C steps with 1 min equilibration time and 1 min signal averaging time per point. A chemical denaturation curve was obtained by measuring ellipticity of a 2 μ*M* protein solution at 222 nm at guanidinium chloride (GdmCl) concentrations between 0 and 6 *M* in PBS, pH 6.5. Every point was averaged over 2 min. Each GdmCl concentration was diluted from an approximately 8 *M* GdmCl in PBS stock solution individually and measured after several minutes equilibration time. The exact concentration of the GdmCl stock solution was determined from the difference ΔN in refractive

index between the approximately 8 *M* GdmCl stock solution and PBS and by applying Equation 3:[50]

$$[\mathrm{GdmCl}] = 57.147 \cdot \Delta N + 38.68 \cdot \Delta N^2 - 91.6 \cdot N^3. \quad (3)$$

After calculating the fraction unfolded (f_U), the data were fit nonlinearly to a dimeric binding model with KaleidaGraph v.4 (Synergy Software) to determine the free energy of unfolding in water $\Delta G_U(H_2O)$ and the cooperativity of unfolding m.[32]

ANS binding

For ANS binding experiments, ANS fluorescence was measured from 400 to 600 nm with 1 nm step size at an excitation wavelength of 370 nm. The signal was integrated for 1 s. Spectra were recorded at 2 μ*M* ANS in the presence or absence of 2 μ*M* protein in PBS, pH 6.5, at 25°C. A PBS spectrum was subtracted as a blank.

Acknowledgment

We thank Dr. Joris Beld and Regula Grüninger-Stössel for help with analytical ultracentrifugation and Dr. Andreas Kleeb for providing pMG211-mMjCM.

References

1. Richards FM (1958) On the enzymic activity of subtilisin-modified ribonuclease. Proc Nat Acad Sci USA 44: 162–166.
2. Anfinsen CB (1973) Principles that govern folding of protein chains. Science 181:223–230.
3. Finn FM, Hofmann K (1965) Studies on polypeptides. XXXIII. Enzymic properties of partially synthetic ribonucleases. J Am Chem Soc 87:645–651.
4. Hamachi I, Hiraoka T, Yamada Y, Shinkai S (1998) Photoswitching of the enzymatic activity of semisynthetic ribonuclease S' bearing phenylazophenylalanine at a specific site. Chem Lett 27:537–538.
5. Nitz M, Mezo AR, Ali MH, Imperiali B (2002) Enantioselective synthesis and application of the highly fluorescent and environment-sensitive amino acid 6-(2-dimethylaminonaphthoyl) alanine (DANA). Chem Commun 2002:1912–1913.
6. Wildemann D, Schiene-Fischer C, Aumüller T, Bachmann A, Kiefhaber T, Lücke C, Fischer G (2007) A nearly isosteric photosensitive amide-backbone substitution allows enzyme activity switching in ribonuclease S. J Am Chem Soc 129:4910–4918.
7. Michnick SW (2001) Exploring protein interactions by interaction-induced folding of proteins from complementary peptide fragments. Curr Opin Struct Biol 11: 472–477.
8. Pelletier JN, Arndt KM, Plückthun A, Michnick SW (1999) An *in vivo* library-versus-library selection of optimized protein-protein interactions. Nat Biotechnol 17:683–690.
9. Magliery TJ, Wilson CGM, Pan WL, Mishler D, Ghosh I, Hamilton AD, Regan L (2005) Detecting protein-protein interactions with a green fluorescent protein fragment reassembly trap: Scope and mechanism. J Am Chem Soc 127:146–157.
10. Campbell-Valois F-X, Michnick SW, Synthesis of degenerated libraries of the Ras-binding domain of Raf and rapid selection of fast-folding and stable clones with the dihydrofolate reductase protein fragment complementation assay. In: Arndt K., Müller K., Eds. (2007) Protein Engineering Protocols. Totowa (NJ): Humana Press, pp 249–274.
11. Leveson-Gower DB, Michnick SW, Ling V (2004) Detection of TAP family dimerizations by an *in vivo* assay in mammalian cells. Biochemistry 43:14257–14264.
12. Remy I, Wilson IA, Michnick SW (1999) Erythropoietin receptor activation by a ligand-induced conformation change. Science 283:990–993.
13. Laser H, Bongards C, Schuller J, Heck S, Johnsson N, Lehming N (2000) A new screen for protein interactions reveals that the *Saccharomyces cerevisiae* high mobility group proteins Nhp6A/B are involved in the regulation of the GAL1 promoter. Proc Nat Acad Sci USA 97:13732–13737.
14. Raquet X, Eckert JH, Müller S, Johnsson N (2001) Detection of altered protein conformations in living cells. J Mol Biol 305:927–938.
15. Ozawa T, Sako Y, Sato M, Kitamura T, Umezawa Y (2003) A genetic approach to identifying mitochondrial proteins. Nat Biotechnol 21:287–293.
16. Ear PH, Michnick SW (2009) A general life-death selection strategy for dissecting protein functions. Nat Methods 6:813–816.
17. Bloom JD, Labthavikul ST, Otey CR, Arnold FH (2006) Protein stability promotes evolvability. Proc Nat Acad Sci USA 103:5869–5874.
18. MacBeath G, Kast P, Hilvert D (1998) Redesigning enzyme topology by directed evolution. Science 279: 1958–1961.
19. Qiu JX, Petersson EJ, Matthews EE, Schepartz A (2006) Toward beta-amino acid proteins: a cooperatively folded beta-peptide quaternary structure. J Am Chem Soc 128:11338–11339.
20. Horne WS, Price JL, Keck JL, Gellman SH (2007) Helix bundle quaternary structure from alpha/beta-peptide foldamers. J Am Chem Soc 129:4178–4180.
21. MacBeath G, Kast P, Hilvert D (1998) Probing enzyme quaternary structure by combinatorial mutagenesis and selection. Protein Sci 7:1757–1767.
22. Vamvaca K, Butz M, Walter KU, Taylor SV, Hilvert D (2005) Simultaneous optimization of enzyme activity and quaternary structure by directed evolution. Protein Sci 14:2103–2114.
23. Bittker JA, Le BV, Liu JM, Liu DR (2004) Directed evolution of protein enzymes using nonhomologous random recombination. Proc Nat Acad Sci USA 101: 7011–7016.
24. Jäckel C, Kast P, Hilvert D (2008) Protein design by directed evolution. Annu Rev Biophys 37:153–173.
25. Lee AY, Karplus PA, Ganem B, Clardy J (1995) Atomic structure of the buried catalytic pocket of *Escherichia coli* chorismate mutase. J Am Chem Soc 117:3627–3628.
26. Pervushin K, Vamvaca K, Vögeli B, Hilvert D (2007) Structure and dynamics of a molten globular enzyme. Nat Struct Mol Biol 14:1202–1206.
27. MacBeath G, Kast P (1998) UGA read-through artifacts - when popular gene expression systems need a pATCH. Biotechniques 24:789–794.
28. Sasso S, Ramakrishnan C, Gamper M, Hilvert D, Kast P (2005) Characterization of the secreted chorismate mutase from the pathogen *Mycobacterium tuberculosis*. FEBS J 272:375–389.
29. Kast P, Asif-Ullah M, Jiang N, Hilvert D (1996) Exploring the active site of chorismate mutase by

combinatorial mutagenesis and selection: The importance of electrostatic catalysis. Proc Nat Acad Sci USA 93:5043–5048.
30. Ghosh I, Hamilton AD, Regan L (2000) Antiparallel leucine zipper-directed protein reassembly: Application to the green fluorescent protein. J Am Chem Soc 122: 5658–5659.
31. Liu DR, Cload ST, Pastor RM, Schultz PG (1996) Analysis of active site residues in *Escherichia coli* chorismate mutase by site-directed mutagenesis. J Am Chem Soc 118:1789–1790.
32. MacBeath G, Kast P, Hilvert D (1998) A small, thermostable, and monofunctional chorismate mutase from the archaeon *Methanococcus jannaschii*. Biochemistry 37:10062–10073.
33. Vamvaca K, Vögeli B, Kast P, Pervushin K, Hilvert D (2004) An enzymatic molten globule: Efficient coupling of folding and catalysis. Proc Nat Acad Sci USA 101: 12860–12864.
34. Woycechowsky KJ, Choutko A, Vamvaca K, Hilvert D (2008) Relative tolerance of an enzymatic molten globule and its thermostable counterpart to point mutation. Biochemistry 47:13489–13496.
35. Stryer L (1968) Fluorescence spectroscopy of proteins. Science 162:526–533.
36. Roderer K, Kast P (2009) Evolutionary cycles for pericyclic reactions—or why we keep mutating mutases. Chimia 63:313–317.
37. Lee AY, Stewart JD, Clardy J, Ganem B (1995) New insight into the catalytic mechanism of chorismate mutases from structural studies. Chem Biol 2: 195–203.
38. Sasso S, Ökvist M, Roderer K, Gamper M, Codoni G, Krengel U, Kast P (2009) Structure and function of a complex between chorismate mutase and DAHP synthase: efficiency boost for the junior partner. EMBO J 28:2128–2142.
39. Porter JR, Stains CI, Jester BW, Ghosh I (2008) A general and rapid cell-free approach for the interrogation of protein-protein, protein-DNA, and protein-RNA interactions and their antagonists utilizing split-protein reporters. J Am Chem Soc 130:6488–6497.
40. Neuenschwander M, Butz M, Heintz C, Kast P, Hilvert D (2007) A simple selection strategy for evolving highly efficient enzymes. Nat Biotechnol 25:1145–1147.
41. Pelletier JN, Campbell-Valois F-X, Michnick SW (1998) Oligomerization domain-directed reassembly of active dihydrofolate reductase from rationally designed fragments. Proc Nat Acad Sci USA 95:12141–12146.
42. Kent KP, Oltrogge LM, Boxer SG (2009) Synthetic control of green fluorescent protein. J Am Chem Soc 131: 15988–15989.
43. Garcia-Viloca M, Gao J, Karplus M, Truhlar DG (2004) How enzymes work: Analysis by modern rate theory and computer simulations. Science 303:186–195.
44. Kienhöfer A, Kast P, Hilvert D (2003) Selective stabilization of the chorismate mutase transition state by a positively charged hydrogen bond donor. J Am Chem Soc 125:3206–3207.
45. Müller MM, Windsor MA, Pomerantz WC, Gellman SH, Hilvert D (2009) A rationally designed aldolase foldamer. Angew Chem Int Ed Engl 48:922–925.
46. Sambrook J, Fritsch EF, Maniatis T (1989) Molecular Cloning: A Laboratory Manual. Cold Spring Harbor, NY: Cold Spring Harbor Laboratory Press.
47. Gamper M, Hilvert D, Kast P (2000) Probing the role of the C-terminus of *Bacillus subtilis* chorismate mutase by a novel random protein-termination strategy. Biochemistry 39:14087–14094.
48. Laue TM, Shah BD, Ridgeway TM, Pelletier SL (1992) Analytical ultracentrifugation in biochemistry and polymer science. Cambridge, UK: Royal Society of Chemistry.
49. Demeler B, Ultrascan - a comprehensive data analysis software package for analytical ultracentrifugation experiments. In: Scott DJ, Harding SE, Rowe AJ, Eds. (2005) Modern Analytical Ultracentrifugation: Techniques and Methods. Cambridge, UK: Royal Society of Chemistry, pp 210–229.
50. Nozaki Y (1972) The preparation of guanidine hydrochloride. Methods Enzymol 26:43–50.